ChemComm

Accepted Manuscript

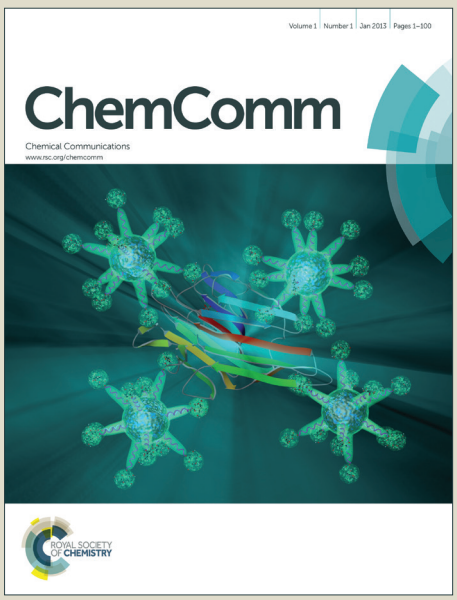

ROYAL SOCIETY OF CHEMISTRY

www.rsc.org/chemcomm

Cite this: DOI: 10.1039/coxx00000x

www.rsc.org/chemcomm

COMMUNICATION

High-k Polymer/Graphene Oxide Dielectrics for Low-Voltage Flexible Nonvolatile Transistor Memories†

Ying-Hsuan Chou, Yu-Cheng Chiu, Wen-Chang Chen*

Received (in XXX, XXX) Xth XXXXXXXXX 20XX, Accepted Xth XXXXXXXXX 20XX

DOI: 10.1039/b000000x

Solution-processable nonvolatile transistor memories on flexible ITO-PEN substrate are demonstrated using the charge storage dielectrics of poly(methacrylic acid) and graphene oxide (PMAA-GO) composites. The hydrogen bonding interaction effectively disperses GO sheets in the high-k PMAA matrix, leading to the control on the memory characteristics. Besides, the fabricated transistor memories have a low operation voltage, a large threshold voltage shift of 5.3–9.4 V, a long retention ability of up to 10^4 s, and good stress endurance of at least 100 cycles.

Among the proposed configurations of organic memory devices, organic field-effect transistor (OFET) type memories have attracted extensive research activities due to their advantages of non-destructive reading, multiple-bit storage, and easily integration in a single transistor.[1-4] The development of nano-floating gate dielectrics[5-7] or conjugated-based polymer electret[8,9] as charges storage layer nonvolatile OFET memories has been widely reported. However, the preparation of metallic nano-dispersed particles and carrier-affinity monomers require relatively complicated processing procedures and polymerization. Although OFET memories using the high-k metal oxide gate dielectrics were developed via expensive atomic layer deposition,[6,10,11] an economically solution-processable high-k polymer dielectrics was rarely explored. Graphene oxide (GO) provides an ideal candidate for large area device applications[12-15] due to the superior electronic properties and easy chemical modification.[16,17] In this paper, we report a soluble-processable high dielectric constant (high-k) poly(methacrylic acid) (PMAA)/GO composites as charge-storage dielectrics for the low-voltage (< 8V) nonvolatile memory devices with a reliable bending stability.

The PMAA/GO composites and crosslinked poly(4-vinylphenol) (cPVP) were employed as charges-storage and blocking layers in p-type 6,13-bis(triisopropylsilylethinyl) pentacene (TIPS-pentacene) based OFET. The incorporation of GO with hydroxyl groups facilitates the hydrogen bonding (Figure 1(a)) with PMAA that allows the well-dispersed GO and enhances the characteristics of the memory devices.

Department of Chemical Engineering, National Taiwan University, Taipei 10617, Taiwan. E-mail: chenwc@ntu.edu.tw

† Electronic Supplementary Information (ESI) available. See DOI: 10.1039/b000000x/

The effects of the GO composition on the morphology and memory characteristics of PMAA-GO3~12 were explored. Note that the digital number of PMAA-GO3~12 composition is the weight percentage of GO blended in PMAA. As shown in Fig. 1(a), the bottom-gate/top-contact OFETs were fabricated on the ITO-PEN (polyethylene naphthalate(PEN)) substrate for the flexible OFET memory. TIPS-pentacene was utilized as the semiconducting layer due to its high solubility in a wide range of solvents and reliable p-channel properties. As shown in Figure 1(b), the peaks at 5.4° are observed from out of plane XRD patterns for both TIPS-pentacene films. It reveals a well-organized molecular structure with the vertical intermolecular spacing of 16.8 Å. The strong peak intensity of the annealed TIPS-pentacene film is resulted from the better intermolecular packing because of the slower solvent evaporation. The AFM image of the solvent-annealed film in Fig. 1(c) indicates a well-arrangement platelet-like morphology, while that of the as-cast one shows a poor-order crystalline structure.

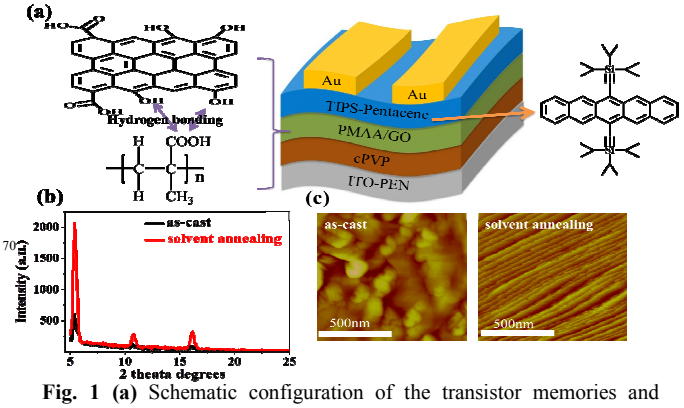

Fig. 1 **(a)** Schematic configuration of the transistor memories and molecular structures of the studied materials; (b) out of plane XRD patterns and (c) AFM topographic images of spin-coated and solvent-annealed TIPS-pentacene thin films.

The GO surface exhibits a wrinkled and aggregated morphology in Fig. 2(a), whereas the Fig. 2(b)~(d) reveal finely dispersed morphologies when the different amount of GO is blended with PMAA. It suggests that the hydrogen bonding interaction[14] leads to the well-dispersion of the GO sheets in the composites. However, some folding-cluster aggregations are observed in the composite with a high-content GO (e.g. PMAA-GO12), due to the strong π-π stacking within GOs. Furthermore, the smooth

surface structure (roughness : 0.2-0.4 nm, Figure S1 of *Supporting Information* (SI)) of PMAA-GO composites spin-cast on the ITO-PEN substrate is obtained (Fig. S1), indicating that the GO is well dispersed in the PMAA.

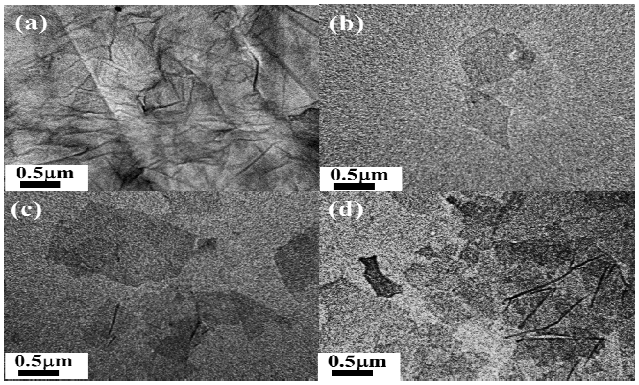

Fig. 2 TEM images of (a) GO, (b) PMAA-GO3, (c) PMAA-GO6, and (d) PMAA-GO12

The high-k dielectric layer (such as PVP[18]) was employed to obtain the low-operating-voltage OFET. Here, we employ the dielectrics of the cPVP, PMAA-GO, and cPVP/PMAA-GO thin films sandwiched between two conductors to measure the leakage currents (Fig. S2, *SI*). The PMAA-GO dielectric exhibits a high leakage current density of around 10^{-2} A/cm^2. The electrons injected form the Au electrode are trapped by the GO sheets and hopping through PMAA-GO composites, resulting in the high conductance state. In contrast, the leakage current density for the cPVP/PMAA-GO thin film evidently decreases to ~10^{-8} A/cm^2 in the bias range of ±3V when the additional cPVP layer (~10^{-7} A/cm^2) is incorporated beneath the PMAA-GO thin film. It clearly suggests that the incorporated cPVP (~100 nm) can block the current passing through the vertical direction effectively due to their cross-linking structure.[19,20] The bilayer cPVP/PMAA-GO dielectric exhibits relatively a high capacitance of 38.3~38.5 nF/cm^2, which is several times higher than that of common polymers, such as PS, PMMA, and PVP.[21] Note that PMAA has a high dielectric constant of 8.1 (Fig. S3).

The field-effect mobility (μ) and I_{on}/I_{off} ratio of the as cast TIPS-pentacene OFET using the PMAA-GO dielectrics are 4.2×10^{-3}~6.2×10^{-3} cm^{2}V^{-1}s^{-1} and ~10^3, respectively, as summarized in Table 1. This relative low mobility and I_{on}/I_{off} performances cannot distinguish the bistable state significantly, leading to the misreading easily in memory device applications. To improve the electrical properties, therefore, the as-cast thin film was placed in a tightly capped bottle containing saturated vapour of toluene for the reorientation and enhancing the crystallinity of TIPS-pentacene. , As summarized in Table 1, the mobility of the TIPS-pentacene OFET using different PMAA-GO dielectric after solvent annealing is enhanced up to 0.22~0.43 cm^{2}V^{-1}s^{-1} with the high I_{on}/I_{off} current over 10^4. They are significantly higher than those of the as-cast films, due to the superior molecular ordering using the solvent annealing.

To elaborate the memory performance, the devices with PMAA/GO were operated by applying appropriate gate pulse (± 8*V*) for one second to lead the shifting on the transfer curves. It thus results in the high- (ON state) and low-conductance (OFF state) states at zero gate bias conditions (V_g = 0 *V*). When applied a positive gate bias (V_g = 8*V* for 1 s), the transfer curves are substantially shifted in the positive direction, served as the writing process, causing a high drain current (ON state). In contrast, the transfer curve is shifted to the negative direction after applied a reverse gate bias (V_g = -8 *V* for 1 s), served as the erasing process. The shifting range on the threshold voltage between writing and erasing plots is defined as the memory windows (ΔV_{th}). Fig. 3 shows the transfer curves of the studied OFET memory devices. The ΔV_{th} of OFET memory devices with PMAA-GO1.5, PMAA-GO3, PMAA-GO6 and PMAA-GO12 as the charge storage layers are 1, 5.9, 7.6, 9.4 and 5.3 V, respectively. Except for the device with PMAA-GO12, the ΔV_{th} increases with enhancing the amount of the GO in the composites. Note that 12 wt% GO in the PMAA matrix exhibits an aggregated structure (Fig. 2(d)) and thus the charges stored in GOs dissipate easily through the cluster between GOs, thus, leading to the smaller ΔV_{th}.

Table 1. Electrical Characteristics of the OFET memory devices (ITO/PEN/c-PVP/PMAA-GO/TIPS-pentacene/Au).

Sample	μ x10^{-3} [a] (cm^{2}V^{-1}s^{-1})	μ x10^{-1} [b] (cm^{2}V^{-1}s^{-1})	I_{on}/I_{off} [b]	Memory window (ΔV_{th}) (*V*)
PMAA-GO0	6.2±0.11	4.3±0.13	2.5×10^4	1
PMAA-GO1.5	5.8±0.08	3.1±0.09	3.1×10^4	5.9
PMAA-GO3	5.4±0.12	2.8±0.11	4.2×10^4	7.6
PMAA-GO6	4.2±0.09	2.2±0.08	3.7×10^4	9.4
PMAA-GO12	4.4±0.10	4.2±0.12	1.3×10^4	5.3

[a] As-cast TIPS-pentacene; [b] After solvent-annealed TIPS-pentacene

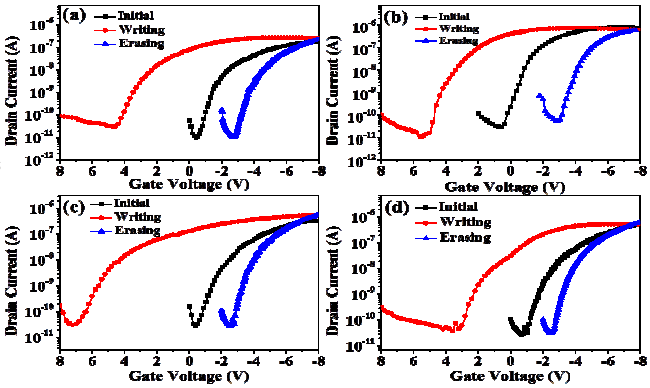

Fig. 3 Transfer characteristics of the OFET memory devices with (a) PMAA-GO1.5, (b) PMAA-GO3, (c) PMAA-GO6 and (d) PMAA-GO12**.**

To elucidate the role of GO in the storage layer, the analogous device using PMAA as dielectric was prepared for comparison. Even though the OFET mobility (0.43 cm^2 V^{-1}s^{-1}) of the PMAA-dielectric device (Fig. S5, *SI*) is similar to that using the PMAA-GO blends, the writing/erasing operations could not shift the threshold voltage, implying the relatively limited charge-storage capability. It suggests that the proposed devices with the bistable transfer curves at V_g= 0 *V* are attributed to the incorporated GO composition. Also, the memory window or storage capability is related as closely as the additive amount of GO and its dispersity in the composites. Importantly, the estimated charge trapping densities[8] (Δn) are 1.36×10^{12}, 1.67×10^{12}, 2.07×10^{12}, and 1.17×10^{12} cm^{-2} for PMAA-GO1.5, PMAA-GO3, PMAA-GO6 and PMAA-GO12, respectively. The numbers of trapped charges

with the magnitude of 10^{12} in the OFET memory devices are comparable to the state-of-the-art nano-floating-gate memory reported in the literature.[5, 11, 14, 22]

The time during which the stored charges are retained in the dielectric layer is defined as the retention time. Fig. 4(a) is the retention time of the devices with different PMMA-GO dielectrics that was measured in a N_2-filled glove box (temperature= 25°C, moisture=0.6 ppm). The ON and OFF states of the device at V_g=0 *V* are maintained for 10^4 s with a high ON/OFF memory ratio of ~10^3-10^4. The devices with PMAA-GO1.5 and PMAA-GO3 show the superior stability and longer retention time for at least 10^4 s since the well-dispersed GOs within the PMAA matrix restrain the release of the trapped charges. However, the retention characteristics of the device with the excessive GO composition (12 wt%) exhibit a rapid dissipation through the pathway of their aggregated region. The above results disclosed the significance of the GO composition and dispersity on the key performances of OFET memory devices, including the memory windows and retention characteristics. The multiple switching stability of the OFET memory device using the PMAA-GO3 dielectric is evaluated through write-read-erase-read (WRER) cycles, as shown in Fig. 4(b). The current is read at 0 *V* with the fixed V_d =-8*V* after repeating the writing/erasing operations with the continuous bias pulses of 8 *V*/ -8 *V*. An ON/OFF memory ratio of more than 10^3 is achieved in the WRER cycles and the responding ON and OFF current could be maintained over 100 cycles stably.

The development of the OFET memory device relies on not only the good data-storage performance but also their bending stability stimulated by external stresses. The threshold voltages under the writing/erasing state, mobility and ON/OFF state of the flexible transistor memories with various bending radii or repeated cycles are investigated. The device using the PMAA-GO3 dielectric is selected to analyze at various curvature radii of 30, 20, 10 and 5 mm. Regardless of the bending condition, no significant alternation in the mobility and memory window is remarkably observed (Fig. 4(c)). Narrow distributions of those parameters emphasize that the switching behaviour is quite stable for the practical applications even under severely compressed condition. Note that the standard deviations calculated from the 15 data of the critical performing parameters are statically analyzed. In addition to flexibility, the reliability of the flexible memories is investigated by measuring the electrical characteristics on the operation of repeating up to 1000 bending cycles. The memory window and mobility show no virtually change during the 1000-bending cycle test (Fig. S6, *SI*). It reveals that the fabricated flexible devices have good mechanical flexibility as well as programmable memory endurance.

In conclusion, a simple solution method to prepare PMAA-GO dielectrics is developed for flexible nonvolatile TIPS-pentacene-based OFET memories with high performance. The introduction of hydrogen bonding in the composites can effectively disperse GO sheets within high-k PMAA matrix. Besides, the fabricated transistor memories have a low operation voltage, a large threshold voltage shift of 5.3–9.4 V, a long retention ability of up to 10^4 s and good stress endurance of at least 100 cycles. The present study suggests that flexible OFET memory devices with a low operation voltage can be achieved using solution-processed high-k polymer composites.

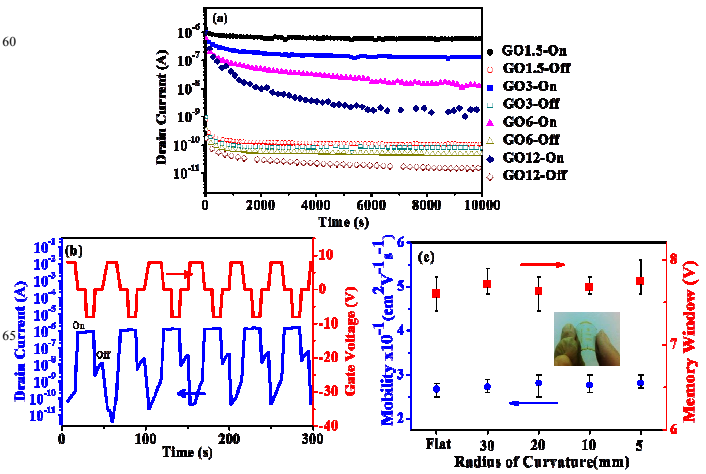

Fig. 4 (a) Retention characteristics of the devices with PMAA-GO dielectrics. (b) Reversible current response to the WRER cycles of the PMAA-GO3 device. (c) Variation of mobility and memory window of the flexible devices with PMAA-GO3 as charges storage layer.

Notes and references

1. Q. D. Ling, D. J. Liaw, C. Zhu, D. S. H. Chan, E. T. Kang and K. G. Neoh, *Prog. Polym. Sci.*, 2008, **33**, 917.
2. P. Heremans, G. H. Gelinck, R. M. Muller, K. J. Baeg, D. Y. Kim and Y. Y. Noh, *Chem. Mater.*, 2011, **23**, 341. 3.
3. J. S. Lee, *J. Mater. Chem.*, 2011, **21**, 14097.
4. Y. L. Guo, C. A. Di, S. H. Ye, X. N. Sun, J. Zheng, Y. G. Wen, W. P. Wu, G. Yu and Y. Q. Liu, *Adv. Mater.*, 2009, **21**, 1954.
5. W. L. Leong, N. Mathews, S. Mhaisalkar, Y. M. Lam, T. Chen and P. S. Lee, *J. Mater. Chem.*, 2009, **19**, 7354.
6. K.-J. Baeg, Y.-Y. Noh, H. Sirringhaus and D.-Y. Kim, *Adv. Funct. Mater.*, 2010, **20**, 224.
7. Q. Wei, Y. Lin, E. R. Anderson, A. L. Briseno, S. P. Gido and J. J. Watkins, *ACS Nano*, 2012, **6**, 1188.
8. J. C. Hsu, W. Y. Lee, H. C. Wu, K. Sugiyama, A. Hirao and W. C. Chen, *J. Mater. Chem.*, 2012, **22**, 5820.
9. Y.-C. Chiu, C.-L. Liu, W.-Y. Lee, Y. Chen, T. Kakuchi and W.-C. Chen, *NPG Asia Mater.*, 2013, **5**, e35.
10. S.-T. Han, Y. Zhou, Z.-X. Xu, L.-B. Huang, X.-B. Yang and V. A. L. Roy, *Adv. Mater.*, 2012, **24**, 3556.
11. S. Kolliopoulou, P. Dimitrakis, P. Normand, H.-L. Zhang, N. Cant, S. D. Evans, S. Paul, C. Pearson, A. Molloy, M. C. Petty and D. Tsoukalas, *J. Appl. Phys.*, 2003, **94**, 5234.
12. S.-T. Han, Y. Zhou, C. Wang, L. He, W. Zhang and V. A. L. Roy, *Adv. Mater.*, 2013, **25**, 872.
13. S. Bertolazzi, D. Krasnozhon and A. Kis, *ACS Nano*, 2013, **7**, 3246.
14. A.-D. Yu, C.-L. Liu and W.-C. Chen, *Chem. Commun.*, 2012, **48**, 383.
15. P. Bhunia, E. Hwang, M. Min, J. Lee, S. Seo, S. Some and H. Lee, *Chem. Commun.*, 2012, **48**, 913
16. X. Huang, Z. Yin, S. Wu, X. Qi, Q. He, Q. Zhang, Q. Yan, F. Boey and H. Zhang, *Small*, 2011, **7**, 1876.
17. D. R. Dreyer, S. Park, C. W. Bielawski and R. S. Ruoff, *Chem. Soc. Rev.*, 2010, **39**, 228.
18. M. E. Roberts, N. r. Queraltó, S. C. B. Mannsfeld, B. N. Reinecke, W. Knoll and Z. Bao, *Chem. Mater.*, 2009, **21**, 2292.
19. H. Klauk, M. Halik, U. Zschieschang, G. Schmid, W. Radlik and W. Weber, *J. Appl. Phys.*, 2002, **92**, 5259.
20. S. H. Lim, J. Kim, S.-g. Lee and Y. S. Kim, *Chem. Commun.*, 2010, **46**, 3961.
21. K.-J. Baeg, Y.-Y. Noh, J. Ghim, B. Lim and D.-Y. Kim, *Adv. Funct. Mater.*, 2008, **18**, 3678.
22. M. Kang, K.-J. Baeg, D. Khim, Y.-Y. Noh and D.-Y. Kim, *Adv. Funct. Mater.*, 2013, **23**, 3503.